

Research Article

Open Access



Soft Schottky diodes for skin-interfaced electronics enabled by entirely soft components

Donghyung Shin^{1, #} , Sehyun Kim^{1, #} , Haechan Park¹, Yeeun Kim¹, Myeonghyeon Na¹, Daeun Kim¹,
Kyoseung Sim^{1, 2, *} 

¹Department of Chemistry, Ulsan National Institute of Science and Technology (UNIST), Ulsan 44919, Republic of Korea.

²Center for Wave Energy Materials, Ulsan National Institute of Science and Technology (UNIST), Ulsan 44919, Republic of Korea.

[#]Authors contributed equally.

* **Correspondence to:** Prof. Kyoseung Sim, Department of Chemistry, Ulsan National Institute of Science and Technology (UNIST), 50, UNIST-gil, Ulsan 44919, Republic of Korea. E-mail: kyos@unist.ac.kr

How to cite this article: Shin D, Kim S, Park H, Kim Y, Na M, Kim D, Sim K. Soft Schottky diodes for skin-interfaced electronics enabled by entirely soft components. *Soft Sci* 2024;4:22. <https://dx.doi.org/10.20517/ss.2024.03>

Received: 31 Jan 2024 **First Decision:** 8 Mar 2024 **Revised:** 15 Mar 2024 **Accepted:** 29 Mar 2024 **Published:** 31 May 2024

Academic Editors: Zhifeng Ren, Sang Min Won **Copy Editor:** Dong-Li Li **Production Editor:** Dong-Li Li

Abstract

Soft electronics have achieved significant development, attracting substantial interest due to their promising potential as a dominant form of future electronics. In this rapidly evolving field, the fully soft Schottky diode plays a critical role as a fundamental building block for electronic circuitry systems. These systems, constructed entirely from soft materials, can tolerate various mechanical deformations when interfaced with human skin, making them ideal for use in health monitoring systems and interactive human-machine interfaces. In this study, we introduce a Schottky diode fabricated entirely from soft materials using a facile solution process, further enabling all-printing fabrication systems. Utilizing the mechanical softness of poly(3,4-ethylenedioxythiophene) polystyrene sulfonate-based soft electrode, poly(3-hexylthiophene) nanofibril composite soft semiconductor, and liquid metal, we successfully fabricated a fully soft Schottky diode. This diode exhibits exceptional electrical characteristics even under various mechanical deformations, showcasing the high durability of the device. We have further developed fully soft rectifiers and logic gates, highlighting the versatility of our study. By incorporating these devices with a piezoelectric nanogenerator in a skin-interfaced energy harvesting system, they exhibit sufficient capability for rectification, ensuring a stable power supply as part of a power supply management system. This approach offers substantial potential for future skin-interfaced electronics, paving the way for advanced wearable technology.

Keywords: Soft Schottky diode, skin-interfaced electronics, fully soft electronics, soft full-wave bridge rectifier



© The Author(s) 2024. **Open Access** This article is licensed under a Creative Commons Attribution 4.0 International License (<https://creativecommons.org/licenses/by/4.0/>), which permits unrestricted use, sharing, adaptation, distribution and reproduction in any medium or format, for any purpose, even commercially, as long as you give appropriate credit to the original author(s) and the source, provide a link to the Creative Commons license, and indicate if changes were made.



INTRODUCTION

The field of skin-interfaced electronics has gained considerable attention in recent years, recognized for its potential to revolutionize society and daily life^[1-5]. These devices offer groundbreaking applications, including health monitoring^[6-9], enhanced user experiences^[10-12], and human-machine interfaces^[13-15]. Most notably, the development of soft diodes is pivotal in advancing these technologies, owing to their crucial role in rectification, signal clipping, switching, and various other functions within electronic systems^[16,17]. Particularly, soft diodes made entirely of soft electronic materials, also known as fully soft diodes, offer significant advantages for seamlessly integrating electronics with the soft human body^[18-20], clearly surpassing traditional diodes whose brittle and rigid nature results in a mechanical mismatch with soft tissues. These advantages are especially notable when compared to devices that employ structural engineering with non-soft elements, particularly in terms of simplifying the complexity of the device fabrication processes such as deposition, lithography, and annealing.

Although there have been efforts to develop flexible diodes for wearable electronics^[19,20], these endeavors have encountered significant challenges. Primarily, these challenges stem from the complex nature of the manufacturing process and the inherent non-softness of materials, which fail to meet the specific requirements of skin-interfaced electronic devices. To address these issues, significant advancements have been reported, such as fabricating intrinsically stretchable polymer diodes^[19,21] and developing fully rubbery Schottky diodes^[22]. However, fabricating these devices involves either multiple layers, leading to cumbersome manufacturing processes, or the laborious task of embedding silver nanowires into elastomers. These complexities ultimately limit their scalability and cost-efficiency. Hence, there is an urgent need to streamline the fabrication of fully soft diodes. Simplifying this process would not only increase their availability but also enhance their effectiveness and usefulness in applications involving skin-interfaced electronics.

Here, we have successfully developed a fully soft Schottky diode composed entirely of soft electronic materials. This diode incorporates a eutectic liquid metal alloy, specifically gallium-indium, as the cathode, a poly(3-hexylthiophene) nanofibril (P3HT-NF) and elastomer-based composite as the *p*-type soft semiconductor, and soft poly(3,4-ethylenedioxythiophene) polystyrene sulfonate (PEDOT:PSS) as the anode. The strategic selection of these materials was based on their respective energy levels, which are crucial for forming appropriate contacts. Specifically, a Schottky contact is formed at the interface between the cathode and the semiconductor, and an Ohmic contact is established at the interface between the anode and the semiconductor, thereby enabling the functional characteristics of diodes. Furthermore, all components can be formed through a solution process, which allows a facile fabrication process of the diode, thereby enhancing scalability and cost-efficiency. The fabricated fully soft Schottky diodes exhibit impressive electrical characteristics, demonstrating a forward current density of 2.01×10^3 A/cm² at 3 V and a notable rectification ratio (RR) of 6.15×10^4 at ± 3 V. The devices retain their electrical performance even when subjected to mechanical strains of up to 30%. Moreover, we have progressed in developing fully soft rectifiers and logic gates using these fully soft Schottky diodes. Impressively, these components showcase sufficient electrical characteristics even under a tensile strain of 30%. Expanding on this technology, we have further demonstrated a skin-interfaced energy harvesting system, achieved by integrating a piezoelectric nanogenerator (PENG) with a fully soft diode-based full-wave bridge rectifier. This system reliably offers a self-powering process for skin-interfaced electronics that require direct current (DC) power. The development of a fully soft diode, enabled by a simple process and device structure, along with integrated circuits, has yielded encouraging results. This advancement potentially facilitates the future progression of fully soft, skin-interfaced electronic systems.

EXPERIMENTAL

Materials

PEDOT:PSS (Heraeus Clevis PH1000) was purchased from Ossila. Polyethylene glycol 400 (PEG) was obtained from Thermo Fisher Scientific. Dimethylsulfoxide (DMSO; > 99.9%), Tergitol 15-s-9 (tergitol), toluene (> 99.5%), regioregular poly(3-hexylthiophene-2,5-diyl) (P3HT; MW = 50,000-100,000), anhydrous dichloromethane (DCM; > 99.8%), and gallium-indium eutectic (EGaIn) were acquired from Sigma Aldrich. Polydimethylsiloxane (PDMS; Sylgard 184) came from Dow-Corning. Styrene-ethylene-butylene-styrene (SEBS, G1657) was purchased from Kraton polymers. Tween 80 was obtained from Duksan Chemicals. Fast-drying silver paint (160040-30) was purchased from Ted Pella.

Preparation of the soft PEDOT:PSS solution

The soft PEDOT:PSS electrode was prepared by initially mixing PEDOT:PSS with DMSO in a weight ratio of 4% to enhance conductivity^[23]. This mixture was then blended with tergitol and PEG in a weight ratio of 100:1:8. Subsequently, the solution was stirred vigorously for 30 min at room temperature.

Preparation of the P3HT-NFs/PDMS composite solution

P3HT was dissolved in DCM to form a 4 mg/mL solution at 80 °C, then cooled at -25 °C for an hour to yield P3HT-NFs^[24,25]. The P3HT-NFs solution was mixed with PDMS in DCM (80 mg/mL) at a weight ratio of 1:4, producing the P3HT-NFs/PDMS composite, which was then stored at -25 °C.

Preparation of the fully soft Schottky diode, bridge rectifier, and logic gates

The fully soft Schottky diode fabrication process began with preparing soft PEDOT:PSS electrodes. The soft electrode was patterned by spin-casting the solution at 500 rpm for 60 s onto an ultraviolet-ozone (UV-O₃) treated SEBS substrate using a polyimide-based shadow mask prepared with a Silhouette Portrait 3 programmable cutting machine. The patterned electrode was subsequently annealed at 100 °C for 30 min. The P3HT-NFs/PDMS composite was then spin-casted onto the electrodes at 500 rpm for 60 s using a polyimide-based shadow mask, followed by annealing at 100 °C for 30 min. EGaIn was applied to the P3HT-NFs/PDMS layer using doctor-blading through a polyimide-based shadow mask. The device fabrication process is schematically illustrated in [Supplementary Figure 1](#). Depending on the type of device, such as a bridge rectifier or logic gates, the soft resistor was fabricated by spin-casting P3HT-NFs/PDMS between the lateral gaps of two soft PEDOT:PSS electrodes, following the same method.

Preparation of the skin-interfaced energy harvesting system

The energy harvesting system was constructed using a commercial PENG and a ceramic capacitor, which were incorporated into the fully soft bridge rectifier. Copper electric cables and the silver paint were used for interconnection to ensure electrical conductivity. For the skin-interfaced system, a soft dry-adhesive film was prepared^[26]. This preparation involved mixing liquid state [10:1 (w/w) ratio of prepolymer to curing agent] with 2.5 wt% Tween 80. To ensure a smooth and consistent adhesive capability, the mixture was thoroughly degassed in a vacuum chamber. Afterward, the PDMS mixture was cast onto a glass slide and placed in a convection oven at 60 °C for two hours, forming the soft dry-adhesive film. Lastly, the integrated system was carefully positioned onto these prepared soft dry-adhesive films.

Characterization of the device and materials

The electrical properties of the fully soft Schottky diode were characterized using a Keithley 4200-SCS semiconductor analyzer, Keysight B2912B, and an LCR meter (E4980A, Keysight Technology Inc.) under mechanical strain, employing a customized stretcher and programmable stretching machine (Bending & Stretchable Machine System, SNM Korea). The rectifiers and OR and AND logic gates were characterized with a RIGOL DG4102 function generator and GW Instek GPP-3323 DC power supply. The output voltage

of the PENG was measured using a Tektronix TBS 2000B digital oscilloscope.

RESULTS AND DISCUSSION

Fully soft Schottky diode and soft electrode

Figure 1A shows a skin-interfaced 5×5 array of fully soft Schottky diodes, consisting of EGaIn, P3HT-NFs/PDMS, PEDOT:PSS, and SEBS, serving as the cathode, semiconductor, anode, and substrate, respectively. Since the device is constructed entirely from soft components, it can be conformally mounted on the human body. Furthermore [Figure 1B], it exhibits excellent mechanical durability under various deformations. Besides the fully soft nature of the diode, a key advantage of our devices is their simple fabrication, based entirely on solution processes such as spin-casting and doctor blading, as schematically illustrated in Figure 1C. This approach offers significant potential for enhanced scalability and low-cost manufacturing. To achieve a sufficiently low surface energy of PEDOT:PSS for uniform electrode formation on the hydrophobic SEBS surface, a surfactant, tergitol [Supplementary Figure 2A], was introduced in PEDOT:PSS^[27,28]. As the weight ratio of tergitol increases, the contact angle of the PEDOT:PSS solution decreases [Figure 1D and Supplementary Figure 2B]. This demonstrates the reduction in surface energy of the solution due to the addition of tergitol. Supplementary Figure 3 clearly shows the excellent coating quality of the PEDOT:PSS film achieved with this addition. Furthermore, PEG was selected as a plasticizer for the PEDOT:PSS-based soft electrode, which is utilized as the cathode in the fully soft diode. PEDOT:PSS has high tensile strength which results in low elongation at break, but adding the plasticizer lowers the tensile strength and allows higher stretchability^[29,30]. Indeed, PEDOT:PSS without PEG demonstrates a dramatic increase in resistance under mechanical strain. In contrast, the PEG addition enables stable resistance under such strain, particularly when the added amount exceeds 8 w/w. This is evidenced by the normalized resistance change in response to mechanical strain [Figure 1E]. While such severe resistance change results from the formation of microcracks in the PEDOT:PSS film without PEG, the film containing PEG shows no obvious physical damage [Figure 1F]. It is noted that the electrical properties of PEDOT:PSS could be further improved by applying additional post-treatment processes to remove the excess insulating phase^[31]. The optimized soft PEDOT:PSS electrode exhibits saturated resistance hysteresis after the second strain cycle [Supplementary Figure 4]. This suggests that the film is excellent for use as a soft electrode in fully soft diodes.

Characteristics of fully soft Schottky diode

Figure 2A shows the energy band diagram of the associated electronic materials, which is critical for operating the fully soft device as a Schottky diode. While a sufficient Ohmic contact is formed between the PEDOT:PSS anode and P3HT, the large energy barrier between the highest occupied molecular orbital (HOMO) level of P3HT and the Fermi level of EGaIn creates the Schottky contact between the semiconductor and the cathode electrode. This allows for suitable device operation as a Schottky diode. As illustrated in Figure 2B, the junction between P3HT and EGaIn causes energy band bending under thermal equilibrium, ensuring a constant Fermi level throughout the system. In this case, the recombination of electrons from EGaIn with holes in P3HT generates a depletion region, inducing a large energy barrier. This barrier is expressed by the built-in potential barrier (V_{bi}), which impedes charge carrier transport through the junction. With a positive potential (forward bias, V_f) applied to EGaIn relative to P3HT, the barrier is reduced ($V_{bi} - V_f$), facilitating charge transport from the HOMO of P3HT to the Fermi level of the metal, enabling electric current flow. Conversely, under reverse bias (V_r ; negative potential to EGaIn relative to P3HT), an increased energy barrier ($V_{bi} + V_r$) at the junction hinders charge transport, thus suppressing current flow. Consequently, the fully soft Schottky diodes exhibit typical diode characteristics [Figure 2C].

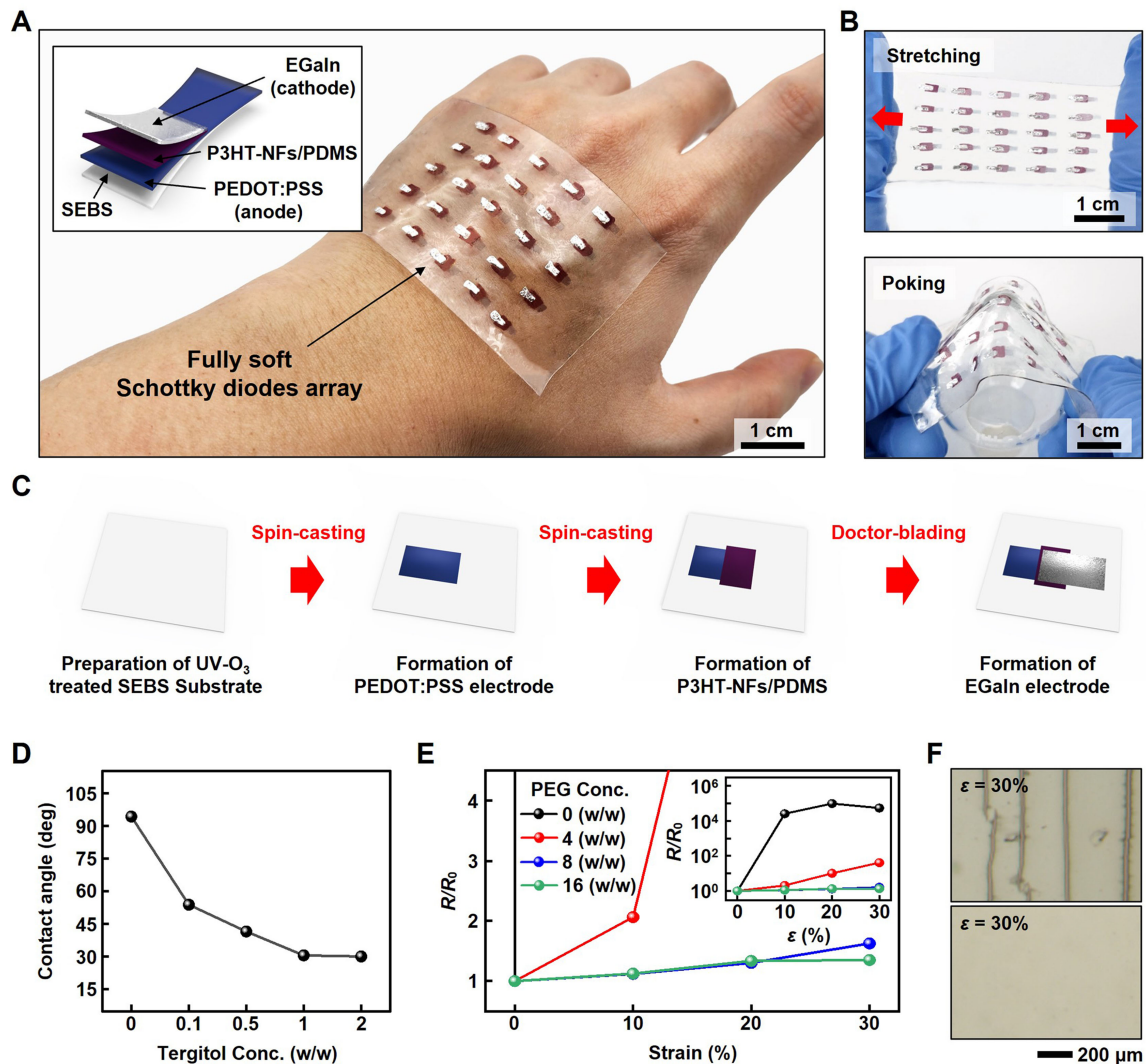


Figure 1. Fully soft Schottky diodes enabled by simple fabrication and soft components. (A) An optical image of a 5×5 fully soft Schottky diodes array (Inset: an exploded schematic illustration of the Schottky diode); (B) Optical images of the diodes array under various mechanical deformation of stretching (top), and poking (bottom); (C) Schematic fabrication process of the fully soft Schottky diode configured in the diodes array; (D) Contact angle-tergitol weight ratio curves of PEDOT:PSS solution (PEDOT:PSS:tergitol, 100:x, w/w) on SEBS substrate; (E) Normalized resistance (R/R_0)-strain curves of PEDOT:PSS electrodes under different PEG weight ratio (PEDOT:PSS:Tergitol:PEG = 100:1:y, w/w) (Inset: overall R/R_0 -strain curve); (F) Microscopic images of PEDOT:PSS in the absence of PEG (PEDOT:PSS:Tergitol = 100:1, w/w) (top), and the presence of PEG (PEDOT:PSS:Tergitol:PEG = 100:1:8, w/w) (bottom) under the mechanical strain of 30%. EGaIn: Gallium-indium eutectic; P3HT-NFs: poly(3-hexylthiophene) nanofibrils; PDMS: polydimethylsiloxane; PEDOT:PSS: poly(3,4-ethylenedioxythiophene) polystyrene sulfonate; UV- O_3 : ultraviolet-ozone; SEBS: styrene-ethylene-butylene-styrene; PEG: polyethylene glycol.

Figure 2D presents a 5×5 array of fabricated fully soft Schottky diodes. These devices exhibit reliable characteristics [Figure 2E], with an average RR of 8.91×10^4 and the highest of 2.92×10^5 [Figure 2F]. The current density under forward bias (J_f) at 3 V averages 1.72 mA/cm^2 and reaches up to 4.32 mA/cm^2 [Figure 2G]. These performance metrics are comparable to those of previously reported soft Schottky diodes^[19,21,22]. The specific current density-voltage (J - V) characteristics of these devices are provided in Supplementary Figure 5.

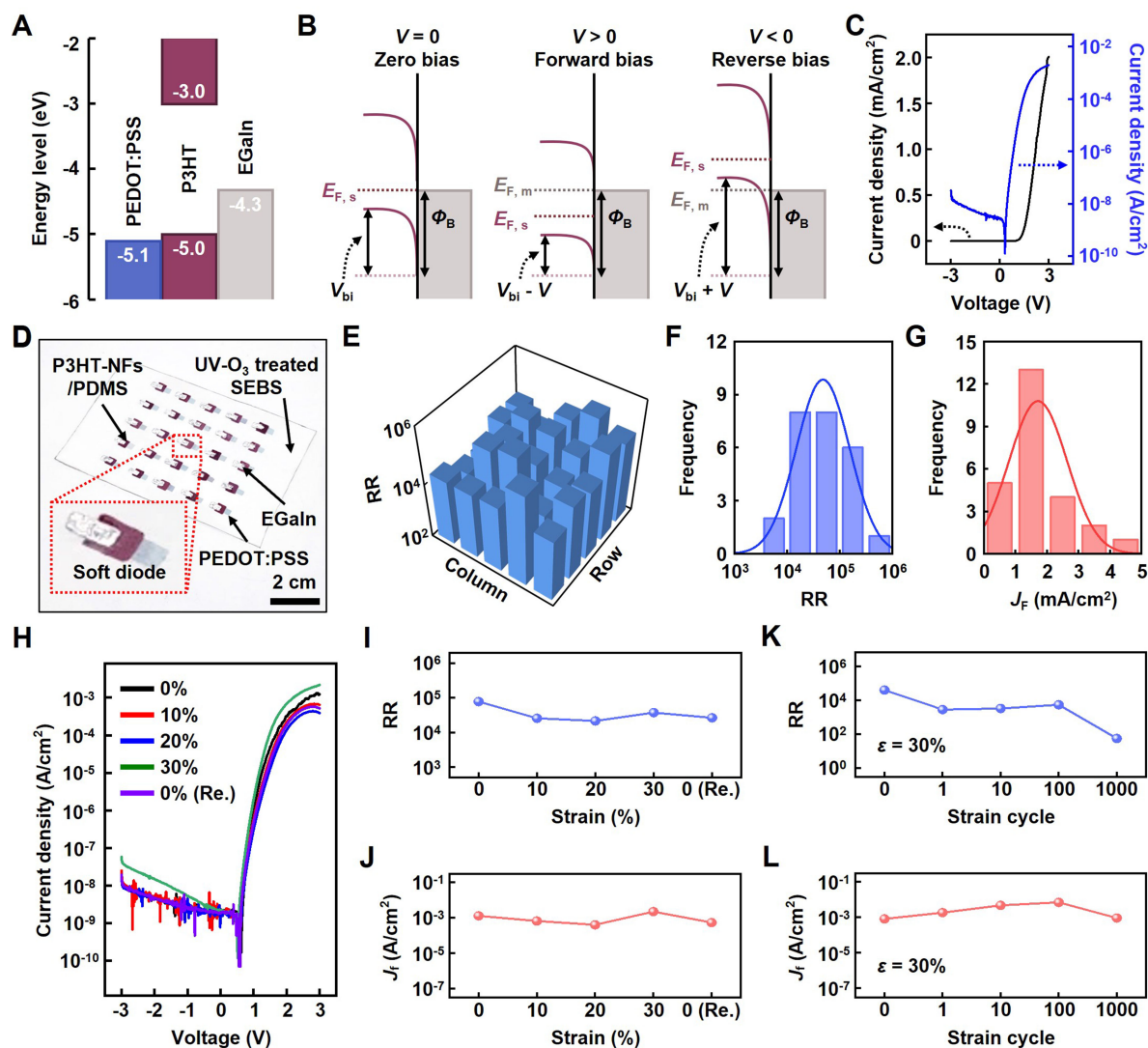


Figure 2. Performance of the fully soft Schottky diode. (A) Energy band diagram of PEDOT:PSS, P3HT, and EGaIn; (B) Energy band diagram upon applied electrical bias; (C) Representative J - V characteristics of the fully soft Schottky diode; (D) An optical image of the diodes array (inset: a magnified optical image of the single device); (E) Calculated RR mapping of the 5×5 diodes array; (F and G) The statistical distribution of RR (F) and J_f (G) of the array; (H) J - V characteristics of the fully soft Schottky diode under the various mechanical strains of 0%, 10%, 20%, 30%, and 0% (released); (I and J) Calculated RR (I) and J_f (J) of the fully soft Schottky diode under the mechanical strains of 0%, 10%, 20%, 30%, and 0% (released); (K and L) Calculated RR (K) and J_f (L) of the fully soft Schottky diode under the repetitive strain cycles at the mechanical strains of 30%. PEDOT:PSS: Poly(3,4-ethylenedioxythiophene) polystyrene sulfonate; P3HT: poly(3-hexylthiophene); EGaIn: gallium-indium eutectic; P3HT-NFs: poly(3-hexylthiophene) nanofibrils; PDMS: polydimethylsiloxane; UV-O₃: ultraviolet-ozone; SEBS: styrene-ethylene-butylene-styrene; RR: rectification ratio; J - V : current density-voltage; J_f : forward current density.

The fully soft nature of these devices ensures reliable operation under mechanical strains of 0%, 10%, 20%, and 30%, and then releasing back to 0% [Figure 2H]. The diodes also show low electrical hysteresis under corresponding mechanical strains [Supplementary Figure 6]. Furthermore, both RR and J values remain stable under tensile strain [Figure 2I and J]. It should be noted that the J under different strains was calculated considering the geometrical deformation of the active area. Additionally, RR and J values remain consistent over 1,000 cycles of 30% stretching and releasing, demonstrating the mechanical robustness of the devices [Figure 2K and L]. The stability of the fully soft Schottky diode under mechanical deformation is

due to its construction from inherently soft materials, a carefully designed structure that evenly distributes strain, and minimized stress concentrations, ensuring intact layer adhesion and consistent electrical performance. These features make the fully soft Schottky diodes suitable for future wearable electronics, which are designed to withstand various forms of mechanical deformation.

Fully soft bridge rectifier

The primary function of a diode as a rectifier is converting alternating current (AC) input into DC output. This function is essential in power supply units, battery chargers, transformers, and numerous consumer electronics^[32]. Considering these requirements, we have developed a fully soft bridge rectifier for full-wave rectification using four fully soft Schottky diodes interfaced by PEDOT:PSS-based soft electrodes [Figure 3A and B]. Figure 3C shows the circuit diagram of this rectifier. Its rectification characteristics, under an input voltage (V_{in}) of ± 10 V at a frequency of 500 Hz, show a reliably rectified output voltage (V_{out}) [Figure 3D]. The voltage drop in the fully soft bridge rectifier is primarily attributed to the forward voltage of the diodes, which occurs when two diodes conduct simultaneously^[33]. Additional voltage drops are caused by the internal resistance of the diodes and by higher load currents^[34]. Figure 3E and F plots the V_{out} of the devices against varying V_{in} amplitudes and frequencies, demonstrating the reliable performance of the rectifier across a wide range of V_{in} . Detailed characteristics are provided in Supplementary Figure 7.

The fully soft bridge rectifier was further characterized under various tensile strains to evaluate its mechanical stability. Figure 3G shows the device under mechanical strain, exhibiting excellent deformability without physical damage. Figure 3H presents the rectification results at ± 10 V input and 500 Hz frequency under mechanical strains of 0%, 30%, and 0% (released). The V_{out} values were maintained without significant degradation, highlighting the robustness of the device under mechanical strain. Figure 3I and Supplementary Figure 8 show V_{out} corresponding to different input frequencies at a constant V_{in} of ± 10 V under 0, 30, and 0% (released) mechanical strains. These results confirm that the fully soft bridge rectifier operates effectively under various electrical conditions and can withstand mechanical strain up to 30%, making it suitable for diverse applications in wearable and skin-interfaced electronics.

Fully soft OR and AND logic gates

The logic gates are crucial components in various electronic circuit systems, providing Boolean functions essential for digital systems^[35,36]. Thus, we further demonstrated the functionality of fully soft logic gates, specifically OR and AND gates, based on fully soft Schottky diodes. The functional verification of the logic gates was conducted by applying biases of 0 and 3 V to the input voltages ($V_{in,A}$ and $V_{in,B}$) of the diodes, representing logic input states of 0 and 1, respectively. Figure 4A and B illustrates the schematic and circuit diagram of the fully soft OR gate, respectively. Notably, the device exhibits exceptional mechanical endurance [Figure 4C]. The electrical characteristics of the fully soft OR gate were evaluated under mechanical strains of 0, 30, and 0% upon release [Figure 4D-F]. These results confirmed that a logic output state of 0 was consistently observed when both $V_{in,A}$ and $V_{in,B}$ were set to a logic input state of 0. In contrast, applying a logic input state of 1 to either one or both diodes resulted in a logic output state of 1, regardless of mechanical strain. Additionally, Figure 4G and H presents the schematic illustration and circuit diagram of the fully soft AND gate. The optical images of the devices, both with and without mechanical strains [Figure 4I], highlight their soft and deformable nature. The electrical operation of the AND gate is presented in Figure 4J, demonstrating that the logic output state is 1 only when both logic input states are 1. This device maintained its logic gate functionality even under a 30% mechanical strain and after the strain was released [Figure 4K and L]. The results from these fully soft logic gates, including their mechanical stability in standard logic operations, are summarized in truth tables provided in Supplementary Figure 9. These comprehensive analyses underscore the robust and reliable functionality of these fully soft logic gates, even under variable mechanical stresses.

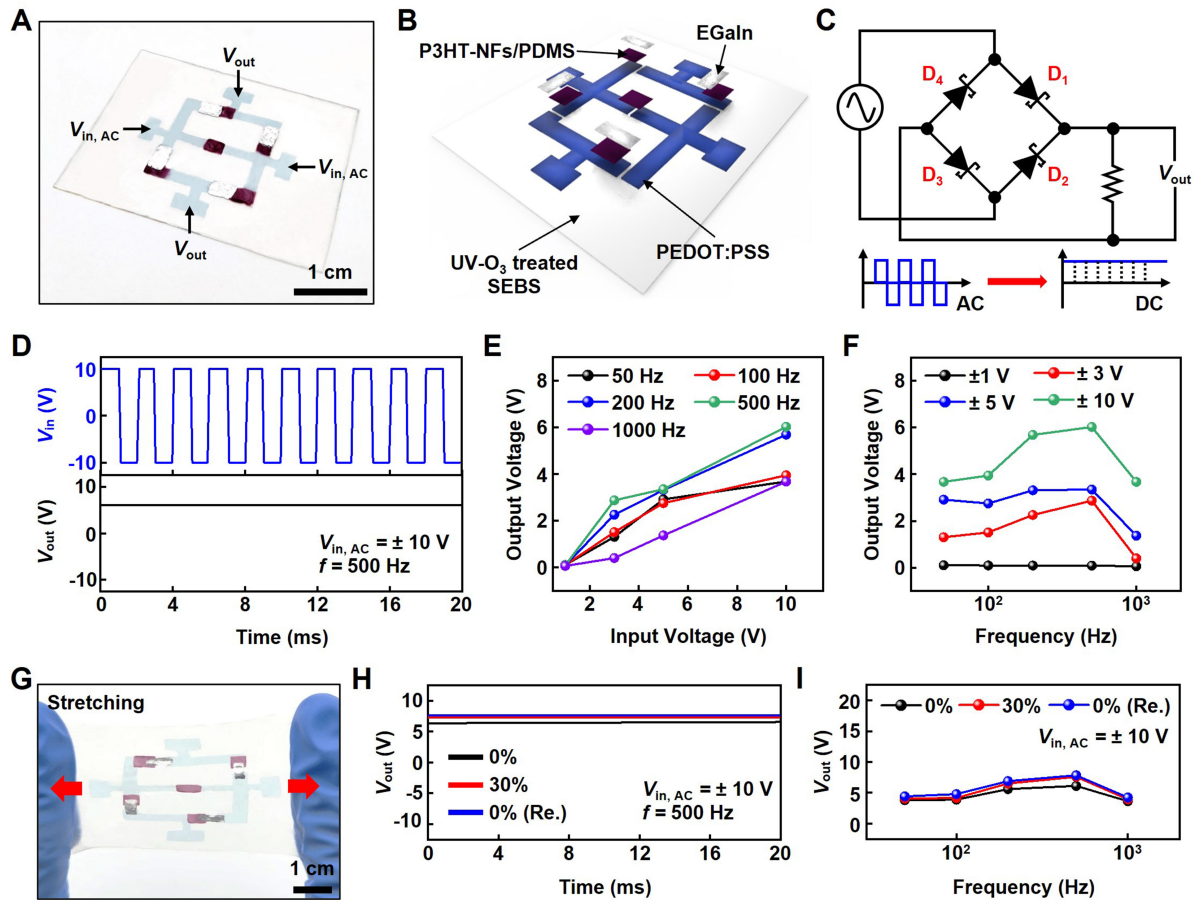


Figure 3. Fully soft bridge rectifier. (A) An optical image of the fully soft bridge rectifier; (B) Schematic exploded view of the fully soft bridge rectifier; (C) Circuit diagram of the bridge rectifier; (D) Rectified V_{out} of the fully soft bridge rectifier under V_{in} of ± 10 V at a frequency (f) of a 500 Hz; (E) V_{out} - V_{in} curves of the fully soft bridge rectifier with various f of 50, 100, 200, 500, and 1,000 Hz; (F) V_{out} - f curves of the fully soft rectifier with various V_{in} of ± 1 , ± 3 , ± 5 , and ± 10 V; (G) An optical image of the fully soft bridge rectifier under the mechanical stretching; (H) Time-dependent characteristic V_{out} curves of the fully soft bridge rectifier under mechanical strains of 0, 30, and 0% (released) ($V_{in} = \pm 10$ V, $f = 500$ Hz); (I) V_{out} - f curves of the fully soft rectifier at $V_{in} = \pm 10$ V. V_{in} : Input voltage; V_{out} : output voltage; P3HT-NFs: poly(3-hexylthiophene) nanofibrils; PDMS: polydimethylsiloxane; UV- O_3 : ultraviolet-ozone; PEDOT:PSS: poly(3,4-ethylenedioxythiophene) polystyrene sulfonate; AC: alternating current; DC: direct current.

Skin-interfaced energy harvesting system

In the realm of wearable technologies, a reliable power supply plays a critical role in ensuring consistent device operation. Owing to the significant inconvenience caused by frequent charging requirements for energy storage devices, harvesting energy from daily activities has gained substantial interest as a sustainable power source^[37,38]. A PENG is one of the promising devices for this purpose, as it efficiently generates electrical power by converting mechanical energy from sources such as vibrations or pressure^[39,40]. However, the AC power generated by PENGs is not immediately suitable for charging batteries or operating wearable electronics. Therefore, an appropriate rectifier is essential. Considering its importance, we have further demonstrated a skin-interfaced energy harvesting system that integrates a PENG with a fully soft diode-based full-wave bridge rectifier. This system seamlessly interfaces with the skin [Figure 5A]. The schematic exploded view of the system is illustrated in Figure 5B, and detailed system interfaces are presented in Supplementary Figure 10. The output voltage from the PENG, induced by finger tapping, clearly shows AC potential in the time domain [Figure 5C]. When integrated with the fully soft rectifier, the system produces sufficiently rectified output voltages [Figure 5D]. However, this system alone does not provide a stable and

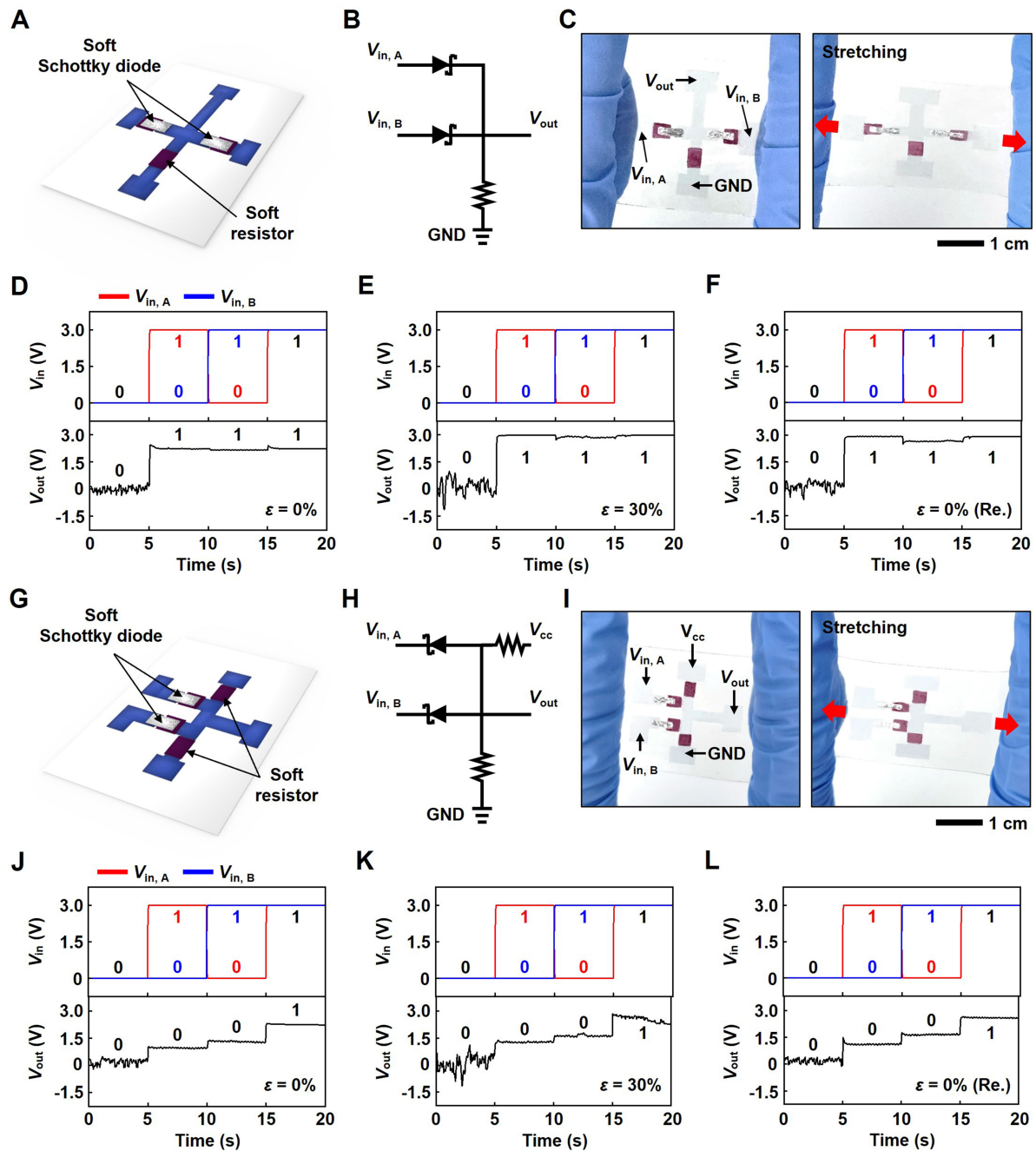


Figure 4. Fully soft logic gates based on the Schottky diode. (A) Schematic illustration of the fully soft OR gate; (B) Circuit diagram of the fully soft OR gate; (C) Optical images of the fully soft OR gate before strain (left) and after strain (right); (D-F) V_{in} and V_{out} of the fully soft OR gate under mechanical strains of 0% (D), 30% (E), and 0% (released) (F); (G) Schematic illustration of the fully soft AND gate; (H) Circuit diagram of the fully soft AND gate; (I) Optical images of the fully soft AND gate before strain (left) and after strain (right); (J-L) V_{in} and V_{out} of the fully soft OR gate under mechanical strains of 0% (J), 30% (K), and 0% (released) (L). V_{in} : Input voltage; V_{out} : output voltage; GND: ground.

smooth DC voltage, which can be further improved by integrating it with a capacitor. In a rectifier circuit, a capacitor functions to smooth out pulsating electric signals by storing electrical energy during voltage peaks and releasing it during troughs, resulting in a more consistent and stable DC voltage^[41-43]. Figure 5E demonstrates that the skin-interfaced energy harvesting system, equipped with both a fully soft rectifier and

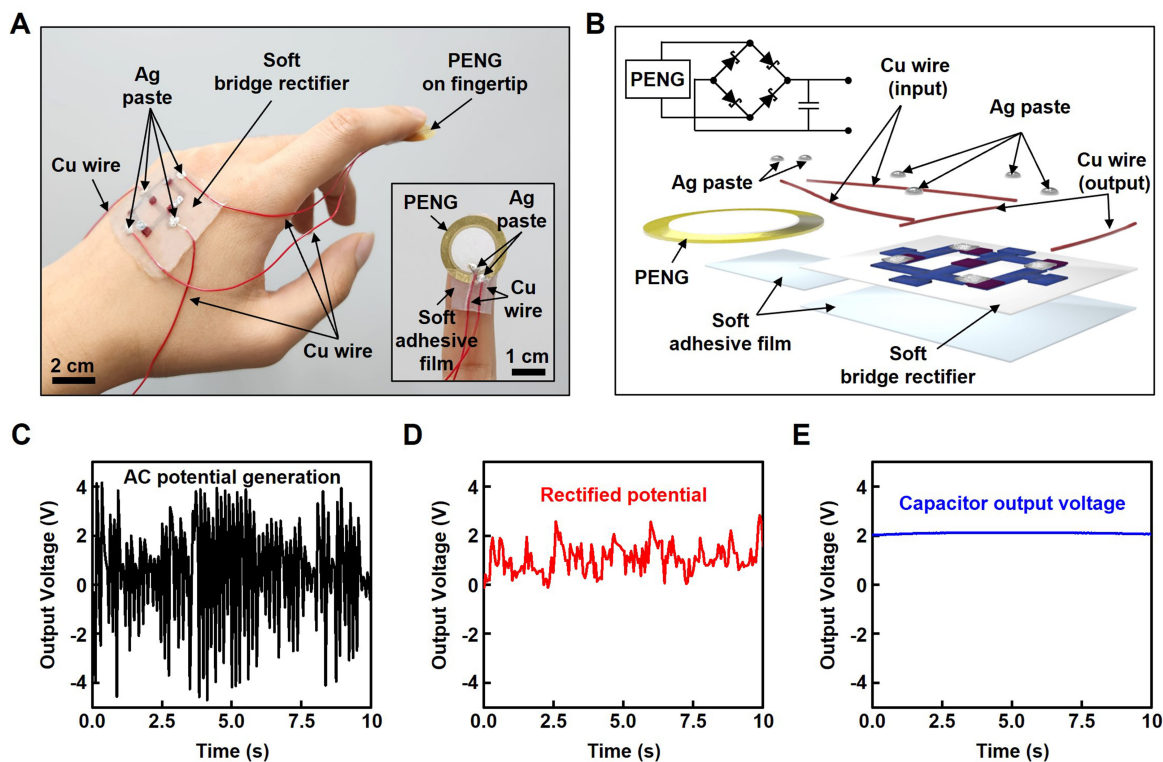


Figure 5. Skin-interfaced energy harvesting system consisting of a fully soft bridge rectifier. (A) An optical image of the skin-interfaced energy harvesting system placed on a human hand; (B) Schematic exploded view of the skin-interfaced energy harvesting system; (C-E) Time-dependent output voltage of the PENG (C), the PENG integrated with a bridge rectifier (D), and the PENG integrated with the capacitor-equipped bridge rectifier by finger tapping (E). PENG: Piezoelectric nanogenerator; AC: alternating current.

a capacitor, yields a stable DC output from the PENG under finger tapping. These results indicate that fully soft Schottky diodes, by efficiently converting mechanical into electrical energy and ensuring a stable/consistent power supply, can be effectively employed in various skin-interfaced electronic systems that require a power management system as an important integral component.

CONCLUSIONS

In conclusion, the fully soft Schottky diode developed in this study demonstrates exceptional electrical characteristics, making it highly suitable for various practical applications in skin-interfaced electronic systems. Comprised entirely of soft electronic materials, this diode demonstrates not only remarkable electrical performance but also exceptional mechanical durability. Unlike many previous works that relied on complex components or labor-intensive fabrication processes, our device offers a streamlined, solution-based process suitable to further all-printing fabrication techniques. This significant advancement addresses key challenges in scalability and cost-efficiency in producing such devices. The fully soft Schottky diodes maintain their electrical integrity even under mechanical strains and repeated stretching cycles, highlighting their robustness. These characteristics enable the extension to fully soft rectifiers and logic gates, showing considerable promise for developing wearable electronics through efficient AC to DC conversion and the execution of Boolean operations. Moreover, successfully integrating these diodes with a PENG in a skin-interfaced energy harvesting system further shows their versatility and capacity for powering electronic devices. This innovation in fully soft electronics paves the way for the future development of advanced skin-compatible electronic systems. This technology holds substantial potential to transform the fields of

wearable technology and human-machine interfaces, opening new avenues for research and applications in this rapidly evolving domain.

DECLARATIONS

Authors' contributions

Conceived the concept and designed the experiments, wrote the manuscript: Shin D, Kim S, Sim K

Prepared materials and fabricated devices: Shin D, Kim S, Park H, Kim Y, Na M

Analyzed the materials: Shin D, Kim S, Park H, Kim D

Characterized the device performance and analyzed the data: Shin D, Kim S, Park H, Kim Y

Designed schematics of the devices: Park H, Na M

All authors reviewed and revised the paper.

Availability of data and materials

The data presented in this study are available upon request from the corresponding author.

Financial support and sponsorship

This work was supported by the research funds of the National Research Foundation of Korea (NRF) grant funded by the Korean Government (NRF-2021R1C1C1007714).

Conflicts of interest

All authors declared that there are no conflicts of interest.

Ethical approval and consent to participate

According to the Korea National Institute for Bioethics Policy, under the Human Subject Research Division, enforcement rule article 13 states that research using only simple contact measuring equipment or observation equipment that does not cause physical changes is exempt from IRB approval. Our work involves simply placing the device on the skin, which does not physically affect humans. Therefore, we do not require Institutional Review Board (IRB) approval.

Consent for publication

Not applicable.

Copyright

© The Author(s) 2024.

REFERENCES

1. Trung TQ, Lee NE. Flexible and stretchable physical sensor integrated platforms for wearable human-activity monitoring and personal healthcare. *Adv Mater* 2016;28:4338-72. [DOI](#) [PubMed](#)
2. Lee Y, Park J, Choe A, Cho S, Kim J, Ko H. Mimicking human and biological skins for multifunctional skin electronics. *Adv Funct Mater* 2020;30:1904523. [DOI](#)
3. Bandodkar AJ, Gutruf P, Choi J, et al. Battery-free, skin-interfaced microfluidic/electronic systems for simultaneous electrochemical, colorimetric, and volumetric analysis of sweat. *Sci Adv* 2019;5:eaav3294. [DOI](#) [PubMed](#) [PMC](#)
4. Liu W, Cheng H, Wang X. Skin-interfaced colorimetric microfluidic devices for on-demand sweat analysis. *npj Flex Electron* 2023;7:43. [DOI](#)
5. Oh SY, Hong SY, Jeong YR, et al. Skin-attachable, stretchable electrochemical sweat sensor for glucose and pH detection. *ACS Appl Mater Interfaces* 2018;10:13729-40. [DOI](#)
6. Lyu Q, Gong S, Yin J, Dyson JM, Cheng W. Soft wearable healthcare materials and devices. *Adv Healthc Mater* 2021;10:e2100577. [DOI](#) [PubMed](#)
7. Patel S, Ershad F, Zhao M, et al. Wearable electronics for skin wound monitoring and healing. *Soft Sci* 2022;2:9. [DOI](#) [PubMed](#) [PMC](#)
8. Kim J, Yoo S, Liu C, et al. Skin-interfaced wireless biosensors for perinatal and paediatric health. *Nat Rev Bioeng* 2023;1:631-47. [DOI](#)

9. Gao W, Emaminejad S, Nyein HYY, et al. Fully integrated wearable sensor arrays for multiplexed in situ perspiration analysis. *Nature* 2016;529:509-14. DOI PubMed PMC
10. Sun G, Wang P, Meng C. Flexible and breathable iontronic tactile sensor with personal thermal management ability for a comfortable skin-attached sensing application. *Nano Energy* 2023;118:109006. DOI
11. Kim NI, Lee JM, Moradnia M, et al. Biocompatible composite thin-film wearable piezoelectric pressure sensor for monitoring of physiological and muscle motions. *Soft Sci* 2022;2:8. DOI
12. Kang YJ, Arafa HM, Yoo JY, et al. Soft skin-interfaced mechano-acoustic sensors for real-time monitoring and patient feedback on respiratory and swallowing biomechanics. *NPJ Digit Med* 2022;5:147. DOI PubMed PMC
13. Sim K, Rao Z, Zou Z, et al. Metal oxide semiconductor nanomembrane-based soft unnoticeable multifunctional electronics for wearable human-machine interfaces. *Sci Adv* 2019;5:eaav9653. DOI PubMed PMC
14. Liu Y, Yiu C, Song Z, et al. Electronic skin as wireless human-machine interfaces for robotic VR. *Sci Adv* 2022;8:eabl6700. DOI PubMed PMC
15. Yu Y, Nassar J, Xu C, et al. Biofuel-powered soft electronic skin with multiplexed and wireless sensing for human-machine interfaces. *Sci Robot* 2020;5:eaaz7946. DOI PubMed PMC
16. Lin S, Shen R, Yao T, et al. Surface states enhanced dynamic schottky diode generator with extremely high power density over 1000 W m⁻². *Adv Sci* 2019;6:1901925. DOI PubMed PMC
17. Bai M, Zhao Y, Xu S, Tang T, Guo Y. Asymmetric bias-induced barrier lowering as an alternative origin of current rectification in geometric diodes. *Commun Phys* 2021;4:236. DOI
18. Ying B, Wu Q, Li J, Liu X. An ambient-stable and stretchable ionic skin with multimodal sensation. *Mater Horiz* 2020;7:477-88. DOI
19. Matsuhsu N, Niu S, O'Neill SJK, et al. High-frequency and intrinsically stretchable polymer diodes. *Nature* 2021;600:246-52. DOI
20. Guo ZH, Wang HL, Shao Y, Li L, Jia L, Pu X. Flexible ionic diodes with high rectifying ratio and wide temperature tolerance. *Adv Funct Mater* 2022;32:2112432. DOI
21. Kim HJ, Chen B, Suo Z, Hayward RC. Ionoelastomer junctions between polymer networks of fixed anions and cations. *Science* 2020;367:773-6. DOI PubMed
22. Jang S, Shim H, Yu C. Fully rubbery Schottky diode and integrated devices. *Sci Adv* 2022;8:eade4284. DOI PubMed PMC
23. Lee I, Kim GW, Yang M, Kim TS. Simultaneously enhancing the cohesion and electrical conductivity of PEDOT:PSS conductive polymer films using DMSO additives. *ACS Appl Mater Interfaces* 2016;8:302-10. DOI PubMed
24. Oh JY, Shin M, Lee TI, et al. Self-seeded growth of poly(3-hexylthiophene) (P3HT) nanofibrils by a cycle of cooling and heating in solutions. *Macromolecules* 2012;45:7504-13. DOI
25. Sim K, Rao Z, Kim HJ, Thukral A, Shim H, Yu C. Fully rubbery integrated electronics from high effective mobility intrinsically stretchable semiconductors. *Sci Adv* 2019;5:eaav5749. DOI PubMed PMC
26. Park H, Na M, Shin D, et al. A skin-friendly soft strain sensor with direct skin adhesion enabled by using a non-toxic surfactant. *J Mater Chem C* 2023;11:9611-9. DOI
27. Campos-Arias L, del Olmo R, Peřinka N, et al. PEDOT:PSS-based screen-printable inks for H₂O₂ electrochemical detection. *Electrochim Acta* 2023;439:141615. DOI
28. Jürgensen N, Pietsch M, Hai X, Schlisske S, Hernandez-sosa G. Green ink formulation for inkjet printed transparent electrodes in OLEDs on biodegradable substrates. *Synth Met* 2021;282:116930. DOI
29. Bontapalle S, Na M, Park H, Sim K. Fully soft organic electrochemical transistor enabling direct skin-mountable electrophysiological signal amplification. *Chem Commun* 2022;58:1298-301. DOI
30. Li P, Sun K, Ouyang J. Stretchable and conductive polymer films prepared by solution blending. *ACS Appl Mater Interfaces* 2015;7:18415-23. DOI
31. Wang Y, Yang L, Shi XL, et al. Flexible thermoelectric materials and generators: challenges and innovations. *Adv Mater* 2019;31:e1807916. DOI
32. Turksoy O, Yilmaz U, Teke A. Efficient AC-DC power factor corrected boost converter design for battery charger in electric vehicles. *Energy* 2021;221:119765. DOI
33. Osiris WG, Farag AAM, Yahia IS. Extraction of the device parameters of Al/P₃OT/ITO organic Schottky diode using *J-V* and *C-V* characteristics. *Synth Met* 2011;161:1079-87. DOI
34. Cohen JE, Horowitz P. Paradoxical behaviour of mechanical and electrical networks. *Nature* 1991;352:699-701. DOI
35. Miyamoto T, Razavi S, DeRose R, Inoue T. Synthesizing biomolecule-based Boolean logic gates. *ACS Synth Biol* 2013;2:72-82. DOI PubMed PMC
36. He T, Ma H, Wang Z, et al. On-chip optoelectronic logic gates operating in the telecom band. *Nat Photon* 2024;18:60-7. DOI
37. Pu X, Hu W, Wang ZL. Toward wearable self-charging power systems: the integration of energy-harvesting and storage devices. *Small* 2018;14:1702817. DOI PubMed
38. Yun J, Kim I, Kim D. Hybrid energy harvesting system based on Stirling engine towards next-generation heat recovery system in industrial fields. *Nano Energy* 2021;90:106508. DOI
39. Yuan L, Xiao X, Ding T, et al. Paper-based supercapacitors for self-powered nanosystems. *Angew Chem Int Ed Engl* 2012;51:4934-8. DOI PubMed
40. Bairagi S, Shahid-ul-islam, Shahadat M, Mulvihill DM, Ali W. Mechanical energy harvesting and self-powered electronic applications of textile-based piezoelectric nanogenerators: a systematic review. *Nano Energy* 2023;111:108414. DOI

41. Jan AA, Kim S, Kim S. A skin-wearable and self-powered laminated pressure sensor based on triboelectric nanogenerator for monitoring human motion. *Soft Sci* 2024;4:10. [DOI](#)
42. Qian F, Liao Y, Zuo L, Jones P. System-level finite element analysis of piezoelectric energy harvesters with rectified interface circuits and experimental validation. *Mech Syst Signal Pr* 2021;151:107440. [DOI](#)
43. Lou Y, Li M, Hu J, et al. Maximizing the energy conversion of triboelectric nanogenerator through the synergistic effect of high coupling and dual-track circuit for marine monitoring. *Nano Energy* 2024;121:109240. [DOI](#)